Title

RIVER MORPHODYNAMIC EVOLUTION UNDER DAM-INDUCED BACKWATER: AN EXAMPLE FROM THE PO RIVER (ITALY).

Running Title

RIVER MORPHODYNAMIC UNDER DAM-INDUCED BACKWATER

Authors

VITTORIO MASELLI[1,2,*], CLAUDIO PELLEGRINI[2], FABRIZIO DEL BIANCO[3], ALESSANDRA MERCORELLA[2], MICHAEL NONES[4], LUCA CROSE[5], MASSIMO GUERRERO[6], JEFFREY A. NITTROUER[7].

[1] University of Aberdeen, Department of Geology and Petroleum Geology, Aberdeen, UK.

[2] Institute of Marine Sciences, ISMAR-CNR, Bologna, Italy.

[3] Consorzio ProAmbiente, Bologna, Italy.

[4] Research Centre for Constructions - Fluid Dynamics Unit, University of Bologna, Italy.

[5] AIPO, Agenzia Interregionale per il Fiume Po, Settore Navigazione Interna.

[6] Department of Civil, Chemical, Environmental and Material Engineering, University of Bologna, Italy.

[7] Rice University, Department of Earth, Environmental, and Planetary Sciences, MS-126, Houston, TX 77005

[*]: Corresponding Author, Email: vittorio.maselli@abdn.ac.uk

Keywords

Po River, backwater, drawdown, lateral river migration, meander, gravel-sand transition.

Highlights

The Isola Serafini dam interrupts the Po River continuity creating a backwater zone that modifies river hydrodynamics for up to 30 km upstream.

Lateral migration rates of meanders reduce downstream, and coarse-grained channel-bars are progressively drowned and reworked over time.

The size of river bed sediment decreases downstream across the backwater zone.

The size of river bedforms increases downstream across the backwater zone.

Dam-induced backwater forced an up-flow shift of the gravel-sand transition.

ABSTRACT

River systems evolve in response to the construction of dams and artificial reservoirs, offering the possibility to investigate the short-term effects of base level oscillations on fluvial architecture. A major effort has been dedicated to the understanding of river response downstream of large dams, where deep channel incisions occur in response to the removal of sediment that is sequestered within the upstream reservoir. Integrating field observations and numerical modelling results, this work quantifies the sedimentary and morphological changes of the Po River (Italy) upstream of the Isola Serafini dam to investigate the impact of dam-induced backwater on river morphodynamics. The construction of a reservoir generates a new base level that forces an upstream shift of alluvial lithofacies and a change in the planform geometry of the river. The lateral migration rate of the channel is up to 45 m/yr upstream of the influence of backwater flow and ca. 10 m/yr at the transition from normal to backwater flow conditions (30 km from the dam). Within this reach, a reduction of the bed shear stress promotes deposition of coarse-grained sediment and the emergence of the gravel-sand transition of the river. The lateral migration of the channel continuously reduces over time, and rates <5 m/yr can be observed within the reservoir backwater zone. This trend is accompanied by the drowning of channel-bars, the reduction of river

competence, and an increase in bedform length. Oscillatory backwater and drawdown surface water profiles can be observed closer to the dam, which are associated with varying low and high discharge events, respectively. While low-flow conditions, persisting for much of the year, allow the deposition of fine-grained sediment, high discharge events not only promote the resuspension and transport of fine material but also the progressive erosion of channel bars and the overall deepening of the thalweg. This study provides a clear picture of the river evolution in response to the construction of a hydropower dam that may be of help in predicting how other fluvial systems will respond to future human interventions. Moreover, the result of how oscillations in base level and backwater/drawdown profiles control river hydro-morphodynamics and sediment transport may provide new insights when reconstructing ancient fluvial and deltaic sequences.

INTRODUCTION

During the last few decades, increasing attention has been dedicated to understanding how fluvial systems evolve in response to changing external forcing and how such signals could be identified in the rock record (Schumm, 1981; Marchetti, 2002; Miall, 2014). Due to a better knowledge of boundary conditions, field studies from late Quaternary systems offer the possibility of investigating the signature of tectonics, climate and/or eustasy in the evolution of fluvial systems (e.g. Blum and Törnqvist, 2000). The integration of direct observations with numerical simulations, and flume experiments, has allowed for a better understanding and ability to predict how allogenic processes influence river hydro-morphodynamics and, consequently, the evolution of subaerial and submarine landscapes (Paola, 2000; Van Heijst and Postma, 2001; Edmonds and Slingerland, 2009; Jerolmack, 2009; Kim et al., 2014; Bufe et al., 2016).

An important step forward towards more accurately modelling connections between fluvial sedimentation and stratigraphy has been the recognition of backwater and drawdown zones upstream of the river mouth (Parker et al., 2008; Hoyal and Sheets, 2009; Lamb et al., 2012), where non-uniform flows occur in response to the river stage (decelerating and accelerating river flow velocities associated with low and high flow conditions, respectively). Numerical simulations and field observations have recently demonstrated that non-uniform flow exerts an important control on the evolution of sediment routing across a range of depositional environments, from the continental realm to coastal and marine areas (Paola, 2000; Moran et al., 2017). For example, depending on the channel depth and river bed slope (Samuels, 1989; Paola, 2000), non-uniform flow may persist for tens to hundreds of kilometres upstream and influence the morphological evolution of the river by controlling the position of the gravel-sand transition (Venditti and Church, 2014), the rate of lateral migration of meander segments (Nittrouer et al., 2012), the river plume hydrodynamics (Lamb et al., 2012), the formation of distributary networks and the evolution of river deltas (Jerolmack and Swenson, 2007; Chatanantavet et al., 2012), and the behaviour of morphodynamic systems (Shaw and McElroy, 2016).

Much of this work has recognized that the backwater profile associated with a prograding river delta promotes sediment aggradation, and consequently reduces rived bed slope and sediment transport capacity which, in turn, enhances downstream fining (Paola and Seal, 1995; Wright and Parker, 2005; Ferrer-Boix et al., 2016; Franzoia et al., 2017). This phenomenon is also evident when a delta progrades into a dam-induced reservoir (Petts, 1979; Church, 1995; Snyder et al., 2004). The study of reservoir sedimentation and of the impact of dams on the evolution of fluvial channels may reveal important insights regarding morphodynamic responses of rivers to external perturbations, such as changes in the elevation of the receiving basin free surface (i.e., air-water interface), or the sequestration of sediment. In particular, a big effort has been devoted to investigating river reaches downstream of large dams (Williams, 1984; Graf, 2006), where the response of fluvial systems has been quantified by coupling observations of planform, cross-sectional and bedform changes with measurements of water and sediment discharge, with the aim to design a set of scenarios for predicting future river evolution (Brandt, 2000; Nones et al., 2013).

This study focuses on a 70-km-long reach of the Po River (Italy) to investigate the upstream effect of a large hydropower dam (Isola Serafini, Fig. 1) on river evolution. The basic idea is to use this trunk of the Po River as a natural laboratory to investigate the short-term effects of base level change and backwater hydrodynamics on fluvial architecture, usually studied in delta distributary channels (Jerolmack and Swenson, 2007). The planform geometry and river bed elevation of the reaches upstream of the dam have been monitored over time since the dam construction, allowing investigations of the river response to such perturbations. By integrating surface observations with sedimentological data (derived from river bed sediment samples and boreholes), hydrological measurements (water elevation and discharge) and numerical simulations, the present study, the first of this genre, aims to quantify how backwater and drawdown flows influence the system morphodynamics and affect sediment partitioning along the channel axis. The results obtained are discussed in the light of understanding the impact of human interventions on fluvial systems and the influence of backwater hydrodynamics on riverine sedimentology, sediment transport processes, channel kinematics and dune dynamics.

STUDY AREA

The Po River arises in the Western Alps and flows roughly West-East for 652 km towards the Northern Adriatic Sea, draining an area of ca. 74,500 km^2 (Fig. 1). The watershed can be divided into three parts on the basis of lithology and maximum elevation: an Alpine sector of crystalline and carbonate rocks (maximum relief 4,500 m above mean sea level, amsl), an Apennine sector mostly composed of sedimentary rocks with high clay content (maximum relief 2,000 m amsl) and a central alluvial area including the Po Plain and the delta (Fig. 1, Amorosi et al., 2016).

The annual hydrograph shows two peaks in discharge, normally in autumn and spring, generated by rainfall and snowmelt, respectively. The mean annual water discharge recorded at the Piacenza gauging station is 959 m^3/s (period 1924-2009; Montanari, 2012), while the total annual sediment and freshwater discharges to the Northern Adriatic Sea are about 13×10^9 kg and 40-50 km^3, respectively (Syvitski and Kettner, 2007; Cozzi and Giani, 2011). On decadal timescales, the water discharge variability mostly reflects a change in the precipitation pattern that bears out a sharpening of the extreme events, as observed in recent years (Zanchettin et al., 2008). For the time interval investigated in this study, an important impact on river dynamics are engineering structures, including embankments for flood control, rip-rap and longitudinal groins (to constrict the channel and facilitate navigation). A direct correlation with the changes observed in the planform geometry and these anthropogenic modifications is difficult to discern (Zanchettin et al., 2008). Moreover, looking over the last five decades, there no evidence of a statistically significant change in the flood hazards along the Po River (Domeneghetti et al., 2015), indicating stationarity of the hydrological series during the evaluated period. Zanchettin et al. (2008) show that extreme discharge events for the Po River (4,800 m^3/s) have a return period of around 50 years, while geomorphologically effective discharges (see Biedenharn et al., 1999), considered to have a return time of approximately one year range from 1,000-2,100 m^3/s for the Po River. Over the time period investigated for this study, there is a noted decrease of the dominant yearly discharge from ca. 2,500 $m^3\ s^{-1}$ to 1,500-1,000 $m^3\ s^{-1}$ (Guerrero et al., 2013).

The Isola Serafini dam, built for hydroelectricity production and completed in 1962, interrupts the continuity of the Po River at ca. 300 km upstream of its mouth (Figs. 1 and 2). The dam has eleven floodgates (width: 30 m each) designed to control the flow through the spillway and to maintain a normal retention level of about 41.5 m amsl (Fig. 3 A), thus forcing the river water surface to oscillate between backwater and drawdown profiles during low and high flows, respectively. Depending on flood intensity, the floodgates may open so as to prevent the river from overflowing, thereby allowing the downstream discharge of water and sediment (Fig. 3 B and C). The construction of the dam affected both upstream and downstream river hydrology, morphology and, consequently, the flux of sediment, nutrients, and dissolved material to the sea (Davide et al., 2003; Surian and Rinaldi, 2003; Bernardi et al., 2013).

In the 250 km reach upstream of the dam (watershed of about $45x10^3\ km^2$), the Po River course changes from a multi-channel braided to single thread meandering, with a bed slope reduction from 1.4‰ to 0.22‰ (Fig. 1). There is an associated fining of river bed sediments from coarse gravel to medium/fine sand (Colombo and Filippi, 2010; Lanzoni, 2012). The present study focuses on the 70 km of river course upstream of the dam, where the modern channel morphology is characterized by a sequence of meander bends both upstream- and downstream-skewed (Fig. 2). This portion of the river is characterized by mean bed slope of 0.215 m/km, sinuosity index of 1.82, water surface elevation between 45 m and 41.5 m amsl, mean and maximum thalweg depths of ca. 6 m and 22 m, respectively, and mean and maximum channel widths of 250 m and 550 m, respectively.

Today, river bathymetry (Fig. 2) is the result of interactions between natural processes and anthropic activities, as the Po River has been significantly affected by human interventions during the last century (Surian and Rinaldi, 2003; Lanzoni et al., 2012). In detail, gravel and sand mining from the river bed, particularly intense in the years between 1960 and 1970, and the construction of hydropower dams in the Alpine tributaries have promoted river bed degradation and a strong decrease in the sediment load, while the creation of longitudinal embankments to prevent flooding of the surrounding alluvial plain and structures used to maintain channel navigation downstream of the Isola Serafini dam have focused flow during dominant discharge events to a single channel (Lamberti and Schippa 1994; ADBPO, 2008). The modern gravel-sand transition has been recognized between the confluence of the Po River with the Tidone and Trebbia tributaries (see Figure 2 for the location of the rivers), where a subtle decrease in slope was created by the deformation of the pre-Quaternary substrate (ADBPO, 2005).

MATERIAL AND METHODS

Field data acquisition and analysis

The planform geometry evolution of the Po River within the study area is quantified by using a combination of orthophotos (years 1954, 1962, 1991) and satellite images (years 2004, 2005, 2014), with the year 1954 (before the construction of the Isola Serafini dam) as a reference for the quantification of river migration rates. Orthophotos were acquired by the IGM (Military

Cartographic Institute) and are available online (http://www.igmi.or/voli). Each photo, at 1:33,000 scale, is rectified as WGS84 UTM33 N in Global Mapper by using 150 control points. Satellite images came from Landsat TM (years 2004 and 2005) and Landsat 8 (year 2014), both with 30 m of spatial resolution (data available at http://earthexplorer.usgs.gov). The river surface area for each year is obtained through image analysis in ArcGIS® by determining the pixel values associated with water and then measuring the total water surface area. This approach may neglect small planimetric variations associated with the river stage, allowing for larger channel widths during high-flow conditions. The position of the river centerline is located by tracking the midpoint perpendicular to river banks derived from the water surface area. Therefore, the centerline is positioned with horizontal errors in the order of few meters, depending on the resolution of the images available. The lateral migration rates are derived by comparing shifts in the river centerline. All the distances presented in this study are reported as kilometres upstream of the Isola Serafini dam.

The thalweg depths for the years 1954 and 2000 presented in figure 2 are derived from the regional topographic surveys of the river channel and the alluvial plain executed by the Interregional Agency for the Po River (AIPO, 2005). The data, referenced to the mean sea level, consists of 14 cross sections ca. 5 km spaced, comprised between the main levees (data available at http://geoportale.agenziapo.it). The modern thalweg depth and the 3D views of the river bed came from a multibeam bathymetric survey performed by AIPO in the years 2004-2005 by using a multibeam echosounder Kongsberg 3002 equipped with a DGPS Racal Landstar (Colombo and Filippi, 2010). Dune lengths are calculated manually from the multibeam bathymetry by measuring the linear distance of two consecutive dune crests; the values are then averaged along 300-m-long sections.

Synthetic borehole logs are derived from the core repository of the Emilia-Romagna Region and Lombardia Region (data available at http://ambiente.regione.emilia-romagna.it and http://www.territorio.regione.lombardia.it, respectively). Samples of river bed sediment, collected by using a Van Veen grab, have been acquired during two campaigns in July and August 2014, both during low flow conditions (Fig. 4). The positioning of the samples has been obtained by using Trimble Marine SPS461 GPS receiver equipped by an internet-based (via GSM) VRS RTK for real-time corrections that provides vertical and horizontal resolutions of 10 cm. Grain-size analyses have been performed with a set of sieves for the >63 µm fraction (from mesh no. 7 to no. 230) and with SediGraph Micromeritics 5120 for finer fractions at ISMAR-CNR sedimentary laboratory. All the samples are treated with 30% diluted H_2O_2 to remove organic matter and washed with distilled water to dissolve salts. Before SediGraph analyses the samples are dispersed in sodium hexametaphosphate and flocculation has been further avoided using mechanical agitation. Grain-size distributions were interpreted using the software Gradistat and are presented via the software graphics (Blott and Pye, 2001).

Water surface elevation data (Fig. 4), converted in water discharge by using the rating curve presented in Cesi (2004), derive from the Piacenza gauging station (source: http://arpa.emr.it, see location in figure 2). The comprehensive information on the water levels measured along the Po River is reported in the Annali Idrologici (http://www.isprambiente.gov.it/it/progetti/acque-interne-e-marino-costiere-1/progetto-annali).

Numerical model

The 70-km-long reach of the Po River investigated in the present study has been simulated by implementing a one-dimensional model from the US Army Corps of Engineers' River Analysis System (US Army Corps of Engineers, 2015). HEC-RAS is a computer model developed by the Hydrological Engineering Center (HEC) that simulates the flow of water in rivers and has been applied in the study area to simulate the impact of backwater zones on the flow velocity and associated bed shear stresses. Fundamental hydraulics handled by the model is the water volume continuity equation and energy equation (De Saint-Venant, 1871), solved using an implicit finite difference scheme (Sturm, 2010). The transport capacity for each grain-size class has been computed by using the Meyer Peter Müller formula and the Van Rijn particles fall velocity (White et al., 1975; Van Rijn, 1984; Gibson et al., 2010). A two-layer approach describing the river bed is applied to simulate armouring and sediment hiding/exposure coefficients, and the resulting particle mobility has been calculated using the active-layer approach (Hirano, 1971). Water flux entrains sediment particles from the active layer composed of coarse particles, which hide the substratum (i.e. inactive layer) of finer sediment, eventually resulting in grains having a reduced mobility.

The starting river profile is described using the 1954 regional topographic survey of the river channel and alluvial plain (AIPO, 2005), interpolating the field measurements to have a maximum fixed spatial resolution of 300 m, necessary to avoid model instability but also to adequately reproduce the hydro-morphodynamics (i.e., celerity of the water flow and changes of the bed elevation) of this reach. With geometry, water depths have been computed assuming changing Manning coefficients between the main channel (n=0.035, quite clean bed) and the floodplains (n =0.025, short grass), based on previous applications (Guerrero et al., 2013; Nones et al., 2018). HEC-RAS computes cross-section averaged shear stresses (Chow, 1959; US Army Corps of Engineers, 2015), while the critical values (Table 1) are computed following the approach proposed by Shields (1936).

A synthetic approach describing the water discharge input at the upstream boundary has been applied aiming to speed up the simulation. This consisted in reproducing the typical annual oscillation that yields two wet and dry periods, as observed in the Po River catchment (Montanari, 2012), and in comparing the numerical outcomes with the observed values. Monthly discharges and their durations at the hydrological station of Piacenza are analysed for the period 1954-2005 and used to calibrate the bed roughness. A sensitivity analysis spanning the period 2000-2005 has been performed to compare the modelling results when applying the synthetic hydrograph (1-month resolution) with the values of water discharge measured at the Piacenza station. The reconstructed hydrograph, spanning the period 1954-2005, points out an overall decreasing in the monthly discharges during wet periods, which reduced from ca. 6,000 to 2,000 $m^3 s^{-1}$ when passing from the first 30 years to the last decades, in accordance with other studies regarding the dominant discharges affecting the Po River morphodynamics (Guerrero et al., 2013). In the simulation, the water level at the downstream end is maintained fixed at 41.5 m amsl in order to reproduce the operation of the gates of the Isola Serafini dam (Fig. 3). The sediment input has been simulated proportional to the flow discharge and adjusted to obtain a 4-5 m lowering of bed level in the first 30 years of the simulated period (i.e., 1954-1984), in agreement with historical data and with the results of previous modelling simulations (Lamberti and Schippa 1994; Guerrero and Lamberti, 2011; Guerrero et al., 2013; Lanzoni et al., 2015).

RESULTS

River bed elevation and channel dynamics

A comparison between thalweg elevations measured in 1954, 2000 and 2005 highlights that the river bed elevation decreases through time in the upstream portion of the study area, between 70 km and ca. 45 km (Fig. 2). Previous studies documented how the lowering of the river bed in this area has been produced by a combination of reduced sediment supply from tributaries and subsequent river bed mining (Marchetti, 2002; Colombo and Filippi, 2010). Between 45 km and 25 km upstream the dam, the bed elevation is generally stable, with slight aggradation observed in some locations (e.g., Section 7 in Fig. 2). Between 25 km and the dam, the thalweg incision progressively increases in the downstream direction: section 14, located just downstream of the dam, shows the highest magnitude of incision, with up to 10 m of river bed degradation (Fig. 2).

A combination of orthophotos and satellite images provide the opportunity to quantify the planform geometry evolution of the Po River after the construction of the dam, highlighting the lateral mobility of channel bars, the stability of river banks and the progressive changes in the water surface area of the channel (Fig. 5). Lateral migration of few hundred meters is recorded in the upstream portion of the river (between 70 and 30 km), where the position of the river centerline changed continuously through time (Fig. 5). In this area, the lateral migration is not accompanied by an increase in channel width, which shows a constant value of ca. 180 m. A closer look at the data highlights that the centerline migration rates are lower in the upstream portion of the river (i.e., up to 25 m/yr between 70 and 55 km), and increase to values of up to 45 m/yr between ca. 55 and 30 km in the years just after dam construction (1954-1962, Fig. 6). Lateral migration rates diminish between 30 and 25 km upstream of the dam, where the river flows near the city of Piacenza, and in its final part upstream of the dam, where the thalweg maintained a consistent position (Fig. 6). In this section the channel, water surface area progressively increases, starting from 30 km upstream of the dam and progressing downstream; the surface area also increased for this section of the river over time, from 1954 to 2014 (Fig. 5). Close to the dam, in meander loop 4, the channel width attains a maximum value of ca. 550 m. Migration rates decrease over time along this 25-km-long section, reaching extremely low values in the final reaches (Fig. 6). The condition of river bank stability is detectable along the 25 km of river course upstream of the dam, which persisted during the entire period investigated, namely between 1954 and 2014 (Figs. 5 and 6).

The planimetric evolution has been accompanied by morphological changes of channel bars, as detected in four snapshots between 1954 and 2004/2005 (Fig. 5). The upstream portion of the river, meander loop 1, shows the most dynamic conditions, with side bars that start to accumulate between 1954 and 1962 (yellow arrows in figure 5), soon after the construction of the dam, with continued growth since then. The point bar, furthermore, is progressively reworked and reshaped, testifying to the dynamism of this reach (orange arrows in figure 5). Moving downstream to meander loop 2, a gradual drowning of the side bars can be observed (between 1962 and 1991, red arrows in figure 5), accompanied by a low degree of point bar reshaping, with banks strengthened by riparian vegetation (blue arrows in figure 5). Farther downstream, side bars disappear soon after dam construction (between 1954 and 1962, in both meander loops 3 and 4, red arrows in figure 5), whereas sandy point bars are drowned faster close to the dam: between 1962 and 1991 in meander loop 3, and between 1951 and 1962 in meander loop 4 (red arrows in figure 5).

River bed sediment and bedforms

River bed sediment samples, collected along the 70 km of the study area, with more detailed sampling in meander loops 1, 3 and 4 (Fig. 7), show the presence of coarse-grained material (D_{50} = 100 mm) only in the upstream portion of the river (along about 40 km): a pebble to cobble river bed develops with patchy sediment distribution and alternate with a more sandy bed, where the average D_{50} is 0.6 mm. Pebbles and cobbles noticeably accumulate where flow velocity increases (i.e., flow thalweg), and finer grained particles are inhibited from depositing (meander loop 1 in figure 7), or at the confluence with the main tributaries entering from the south. At this location, cobbles (sourced from the Apennines) remain in place without transport by the modern Po River (ADBPO, 2005). Cobbles of different lithologies are also found in a few samples farther downstream and are probably materials accumulated during the operations for streambank stabilization. Approaching meander loop 3, sediment samples are almost entirely characterized by sand with a D_{50} between 0.5 mm and 0.3 mm. Finer deposits, with high clay content, are found in low-velocity zones, for example on the inner side of the meander towards the drowned point bar (Fig. 7). Farther downstream, within the final reaches of the river next to the dam (meander loop 4, Fig. 7), bed sediment becomes finer and dominated by silt-size fractions, with an average D_{50} between 0.2 mm and 0.01 mm. This trend is well highlighted by the grain size distribution of the river bed sediment sampled in the thalweg along the final 15 km (Fig. 8). A comparison between aerial views of this final river reach, acquired before and 50 yr after the construction of the dam (1954 and 2004-2005, during low flow conditions), highlights how the downstream decrease in particles size is accompanied by the drowning of the system and the disappearance of coarse-grained channel bars. The stratigraphy of the study area, as highlighted by a series of boreholes (Fig. 9), is characterized by a layer of anthrosol above thick gravel deposits, often amalgamated or alternated with more sandy or clayey sediment. The borehole data support the hypothesis of a gravel-bed river along the entire study area, even where fine-grained sediments are accumulating nowadays, and therefore the presence of coarse-grained channel bars down to the location of the dam (Fig. 9).

The three-dimensional views of the river bed, derived from the multibeam bathymetry, show a variety of depositional and erosional features, both active and remnant. Figure 10 provides a summary of the most common features encountered progressing along the flow direction. Where the river is characterized by shallow depths and coarse-grained material (between 70 km and 45 km), the river bed is almost flat and few detectable bedforms develop ("alpha" and "beta" in figure 10). Farther downstream, fields of transverse, slightly sinuous, sand dunes develop, often showing bifurcation of the crests ("gamma" in figure 10). In the proximity of the dam ("delta" in figure 10), the largest dunes are detected, with heights and lengths on the order of 1 meter and 100 m, respectively. A summary of the mean grain sizes of river bed sediment and mean dune lengths plotted with distance upstream of the dam highlights a progressive change approaching the structure: a decrease in sediment grain size and an increase in dune size (Fig. 11).

Bed shear stresses

The 1D numerical model implemented in HEC-RAS simulated water surface profiles and bed shear stress for different river stage conditions (Fig. 12). At low discharge, the river exhibits a typical backwater profile of the M1 type (for mild channel slopes). The water surface slope break during low flows (350 $m^3 s^{-1}$) occurs at a distance of ca. 20 km upstream of the dam (Fig. 12, left). At higher discharges (i.e., 2,100-4,800 $m^3 s^{-1}$, return period of 10-50 years), an accelerated M2 profile can be recognized, and a drawdown of the water profile happens close to the dam (Fig. 12, left). The M1 and M2 profiles observed at different river discharges are linked to different conditions of bottom shear stress: while backwater conditions force a strong reduction in shear stress, and consequently a spatial decrease in sediment transport capacity approaching the dam, drawdown promotes enhanced shear stress for increasing water discharge conditions (Fig. 12, right). Farther upstream, the model shows that the highest bed shear stress is located ca. 45 km for a discharge of 4,800 $m^3 s^{-1}$ (black curve in Fig. 12, right) because of a local increase of the bed slope, followed by a strong reduction moving downstream to 30 km that continues with a low value until

20 km upstream of the dam. In the upper part of the study area, between 70 and 40 km, the model gives values of the shear stress lower than the critical shear stress for gravel-size particles that reflects scarce mobility during low flow conditions. In this trunk of the river, field observations show the presence of cobbles and pebbles alternated with sandy beds (Fig. 7).

In the time interval investigated in this study, a decrease of the yearly dominant discharge from ca. 2,500 $m^3 s^{-1}$ to 1,500-1,000 $m^3 s^{-1}$ has been observed (Guerrero et al., 2013). Given that the dominant (or effective) discharge is the flow that cumulates most of the channel bed sediments (Biedenharn et al., 1999), the intermediate profiles of figure 12 (green and blue) are critical for the long-term watercourse morphodynamics, as reproduced by the HEC-RAS model.

DISCUSSION

The downstream hydrodynamic changes associated with a river entering a standing water body (a reservoir, a lake or the sea) have fundamental implications for sediment transport processes and channel dynamics. In recent years, many efforts have been made to understand how, how much, and how far upstream, the presence of a standing body of water affects the behaviour of the fluvial system itself (Fernandes et al., 2016). The study of anthropogenically modified rivers entering reservoirs and of natural systems flowing into lakes and seas helped in the understanding of the response of rivers to external perturbations (Collier et al., 1996; Grant et al., 2003), the morphodynamics of deltas and estuaries (Jerolmack and Swenson, 2007; Edmonds et al., 2009; Chatanantavet et al., 2012; Lamb et al., 2012; Bolla Pittaluga et al., 2015), and the evolution of continental and coastal landscapes (Edmonds and Slingerland, 2006; Geleynse et al., 2011). Here we use a trunk of the Po River where a backwater/drawdown zone is produced by a reservoir maintained after the construction of a dam; this can be considered a natural laboratory to investigate the morphodynamic evolution under gradually-varied flow conditions, in comparison with the observations made in river systems towards their outlets into oceans (Nittrouer et al., 2012).

Morphological change within the backwater zone

A combination of morphological and sedimentological evidence, coupled with numerical simulations, shows that the backwater zone associated with the Isola Serafini dam extends upstream for ca. 30 km; this value may also be confirmed by applying the backwater length-scale equation $L \approx H/S$ (S: channel bed slope, H: flow depth at the river mouth; Paola, 2000) to the study area, where $H=6$ m and $S=0.000215$. Upstream of backwater influence (between 70 km and 30 km, approximately), the lateral migration rates of the river are high; modelling results show that the shear stresses calculated for this sub-reach are sufficient to transport coarse sand also during moderate flow conditions (1,000-2,000 m^3 s^{-1}, Fig. 12). The transition from normal to backwater flow conditions is marked by a sudden drop in the rates of lateral migration for the meanders (Fig. 6) and by a progressive reduction in the size of river bed sediment (Fig. 11). Modelling results demonstrate that the water surface slope break during low flow (at 350 m^3s^{-1}, Fig. 12) occurs at ca. 22 km upstream of the dam, in agreement with the field observations. Along the final reaches of the Po River and, in particular, close to the Isola Serafini dam, lateral migration rates decrease to extremely low values (< 5m/yr), sandy channel bars are progressively drowned, and the river erodes its bed along the thalweg (Figs. 5, 6 and 7).

To fully understand the morphodynamics of this reach, it is necessary to evaluate the hydrodynamic conditions during both low flow and high discharge events. During low flows, with a water discharge less than 1,000 m^3 s^{-1} that persists for much of the year, a typical M1 water surface profile is observed (Fig. 12, left). This condition generates a drop in the bed shear stress to values below the critical threshold of bed-load transport for silt-sized sediments (Table 1), and is associated with the accumulation of fine-grained material in the channel axis and along channel bars (Figs. 7 and 8). During floods and high-discharge events, conversely, the river transport capacity changes drastically: the normal retention level is maintained at a constant elevation through the opening of the floodgates, producing an M2 water surface profile and the downstream increase in river flow velocity (i.e., 2,100 m^3 s^{-1} and 4,800 m^3 s^{-1}, Fig. 12, right). As shear stress increases, the river becomes erosional, removing fine-grained sediment accumulated during low flow river stages and partially reworking the antecedent coarse-grained channel bed sediment. Modelling simulations highlight that the drawdown condition is reached for water discharges >2,000 $m^3 s^{-1}$, and generates high bed shear stress close to the dam, which promotes coarse-grained sediment transport as bedload (Fig. 12). The condition of low flow discharge and associated backwater profiles persists for much of the year, generating the overall downstream fining of river bed sediment observed in the model simulations, while pulses of coarse-grained material are associated with episodic high discharge events, characterized by a drawdown of the water surface profile.

The backwater/drawdown oscillations occurring during different river stages, first observed by Lane (1957), may help explain the reduction in lateral river migration, the deep incision of the channel thalweg, the formation of armoured beds, and the partial removal of sediment accumulated along the channel bars. Similar processes have been observed in the Teshio River (Ikeda, 1989) and in the Mississippi River (Nittrouer et al., 2012). In this latter example, lateral migration rates decrease from more than 120 m/yr to less than 20 m/yr along the last 600 km upstream of its outlet (Hudson and Kesel, 2000); this has been related to the backwater morphodynamics generated by the impact of the Holocene sea level rise on the river (Nittrouer et al., 2012). In the Lower Mississippi River, a 100-fold increase in sand transport has been observed during high-discharge events associated with an increase in shear stress by a factor of thirteen, compared to low flow conditions (Nittrouer et al., 2011). A decrease in lateral migration rates (Fig. 6) favoured the growth of riparian vegetation on streambanks and channel bars (Fig. 5), promoting stabilization of the river course. In detail, the effect of vegetation on bank stability is twofold, as it increases soil strength through the network of roots and reduces soil moisture content through canopy interception and evapotranspiration (Thorne, 1990; Simon and Collison, 2002; Wickert et al., 2013). Embankment construction for flood protection, introduced during the last few decades, has further increased bankline stability. The reduction of lateral migration coupled with the deepening of the channel towards its outlet may promote a narrowing of the channel belt, which could be preserved in the stratigraphic record of the fluvial deposit. This concept can be useful when interpreting ancient fluvial-deltaic systems, as low values of the width-to-thickness ratio of the channel belt, associated with limited lateral migration rate (e.g., up to few channel widths), may be diagnostic of distributary channels (Gibling, 2006; Blum et al., 2013; Colombera et al., 2016).

Sedimentological changes within the backwater zone

The hydrodynamic behaviour of the Po River throughout backwater/drawdown zones can be quantified not only by considering spatial information such as lateral river migration and channel deepening and widening, but also by examining the morphological evolution of channel bars and the grain size partitioning along the channel axis. Consecutive aerial surveys of the Po River during the last 60 years, since dam-induced backwater was created, show that the point bars and side bars, continuously evolving through time between 70 km and 30 km (Fig. 5), are often accompanied by a lateral migration of the channel through cutbank erosion. Farther downstream, in particular along the 30 km of river upstream of the dam, the establishment of a backwater zone coincides with channel deepening; this arises as repeated oscillations between M1 and M2, associated with the transition between discharge conditions, progressively erodes channel bars and the thalweg (Figs. 2 and 5).

The morphological changes associated with the variation of the river transport capacity are reflected in river-bed grain size data: coarse sediments characterize the upstream portion of the system, with a progressive downstream fining trend observed along the 30 km river reach upstream of the dam. Interestingly, the upstream limit of the backwater zone nearly overlaps with the area where the gravel-sand transition of the river is observed. Pebbles and coarse sand that characterize the river bed in the upstream portion of the study area are gradually veneered by fine sand and silt moving downstream and, close to the dam, where the flow velocity is extremely low, by clay. River bed samples from the drowned point bars in meander loops 3 and 4 (Fig. 7) show, in detail, a coarsening trend towards deeper water, with clay-rich sediment accumulating at the inner point bar (Fig. 7). This scenario is in marked contrast with the morphology of both the meanders observed in 1954 (before the dam), where coarse-grained point bars are subaerially exposed (Fig. 8), and the presence of a gravel-bed river can be deduced by the stratigraphy of the boreholes (Fig. 9). Based on the observations made in meander loops 3 and 4, it is possible to conclude that a fining upward trend, with more frequent mud-drapes, should characterize the vertical sedimentary succession of a point bar where the river enters the backwater zone. This finding may be of consideration when interpreting ancient river deposits at outcrop or sediment-core scales (Shanley et al., 1992; Labrecque et al., 2011).

The change in river hydraulics and bed material composition observed throughout the backwater zone is also reflected by a change in bedform geometry (Fig. 10), specifically, showing a downstream increase in length (Fig. 11). This trend may be connected to a combination of the general fining of bed sediments, and the occurrence of high flow velocity during high-discharge events, as both factors contribute to increasing dune size (Southard and Boguchwal, 1990). It is possible that the large-scale dunes form only during high-discharge events and remain as relict features (i.e., not in flow equilibrium) during subsequent low flow conditions; this type of pattern has been observed along the Yangtze River (Chen et al., 2012). The general trend of downstream increase in dune height, highlighted in figure 10, could also be linked to increasing water depth progressing into the backwater segment. Moreover, the multibeam bathymetric data available in the study area show that the river bed is normally mantled by dunes along straight reaches and within the inner portion of meander bends, while pools and outer banks lack bedforms and are dominated by erosional forms, particularly in the deeper portions. This evidence agrees with the observations from the lowermost Mississippi River, which indicate a lack of bedforms in meander bends where faster flows generate sediment suspension and inhibit bedform development (Nittrouer et al., 2008). Future investigations supported by repeated multibeam bathymetric surveys could help provide a detailed understanding of how backwater and drawdown hydrodynamics control the evolution of the river bed, including the formation of bedforms as is coupled to downstream sediment transport.

Implications for the gravel-sand transition of the river

It is widely recognized that the size of bed sediments in alluvial rivers decreases downstream (Church and Kellerhals, 1978; Frings, 2008; Franzoia et al., 2017), and among such variations the transition from gravel to sand is a fundamental boundary in the fluvial geomorphology, as it marks key changes in river planform geometry. Two processes have been proposed to explain sediment downstream fining and the emergence of a gravel-sand transition in a river (i.e., grain breakdown and selective transport; Schumm and Stevens, 1973; Hoey and Ferguson, 1994; Ferguson et al., 1996; Ferguson, 2003), and several studies pointed out the influence of backwater on river capacity as a fundamental mechanism (Sambrook Smith and Ferguson, 1995; Venditti and Church, 2014). The gravel-sand transition in the Po River has been recognized between the confluences with the Tidone and the Trebbia tributaries (Fig. 2), and has been associated to a slight decrease in river bed slope due to the deformation of the pre-Quaternary substrate (ADBPO, 2005). Interestingly, modelling results highlight a strong reduction of the bed shear stress between 40 and 20 km upstream of the dam (Fig. 12), where river hydrodynamics start conveying the backwater effect.

Orthophotos acquired in 1954 indicate that the river, within the study area and farther downstream of the Isola Serafini dam, was characterized by the presence of large point bars, side bars and both vegetated and un-vegetated mid-channel bars (Fig. 8). Conversely, none of these bars are present in the 2004-2005 satellite image along the 30 km upstream of the dam (Fig. 8). The stratigraphy derived from the boreholes shows armoured gravel beds below the modern anthrosol across the entire study area (see ADBPO, 2005 and Fig. 9), suggesting that the channel bars in 1954 (Fig. 8) were probably coarse-grained. Combining such information, it is possible to argue that before the construction of the dam, when the base level of the river was at sea level, the gravel-sand transition was located kilometres downstream with respect to the modern position. Therefore, the new base level created by the reservoir forced retrogradation of alluvial lithofacies and a change in the channel pattern (Schumm, 1993), as suggested by the erosion and drowning of the channel bars (Fig. 8). In addition, the emergence of the gravel-sand transition at the upstream limit of the backwater zone, where a strong decrease in bed shear stress promotes the deposition of coarse-grained sediment, suggests the dam-induced backwater as a primary control on its location. This result adds value to the importance of the backwater effect in establishing not only the downstream evolution of the river impacting the genesis of the distributary channel network of the delta (Jerolmack and Swenson, 2007; Edmonds and Slingerland, 2009; Chatanantavet et al., 2012; Lamb et al., 2012; Bolla Pittaluga et al., 2015), but also the river morphodynamics and associated lithofacies for tens of kilometres upstream. The data presented, moreover, may be further discussed in the light of better understanding the time-response of alluvial river systems to external perturbation and how changes of the river dynamics may be preserved in the sedimentary record.

CONCLUSIONS

The combination of field observations and numerical modelling simulations show that the effect of the dam-induced backwater on river hydro-morphodynamics propagates upstream for up to 30 km. The dam interrupts the river continuity and generates a new base level, forcing a retrogradation of alluvial lithofacies and a change in the planform geometry. At the transition from normal to backwater flow, a strong decrease in water surface slope and associated bed shear stress promotes the deposition of coarse-grained material and the emergence of the gravel-sand transition of the river. Along the 30-km-long reach of the river affected by backwater, lateral migration rate of the meanders progressively reduces approaching the dam and is accompanied by a general fining of river bed sediment and an increase in dune length. Closer to the dam, M1 and M2 water surface profiles are modelled in response to low-flow and high-discharge events, respectively. During low-flows, which persist for much of the year, the bed shear stress is low enough to promote deposition of fine-grained sediment (up to clay size), and during high-flow events, a significant drawdown can be observed, which enhances bed shear stress and promotes the removal of the fine-grained material, resulting in the progressive erosion of the channel bars and the overall deepening of the river thalweg.

In essence, this study shows the evolution of the upstream portion of a river after the construction of a dam and highlights the effects of base level rise, backwater and drawdown processes in controlling fluvial hydro-morphodynamics and sediment transport processes. These concepts, applied to source to sink studies of continental margin evolution, may provide better understanding of how far upstream a change in base level may affect fluvial architecture and facies, and of how M1 and M2 oscillations in the backwater zone govern the evolution of channel belts, control sediment yield to the receiving basin and, ultimately, disperse material to depositional basins.

ACKNOWLEDGEMENTS

We would like to thank AIPO for giving the access to multibeam bathymetric data and the permission to display part of them. We thank Patrizia Giordano for the help in grain size analysis, Stefano Miserocchi for the support in organizing the field activity. This manuscript strongly benefited from the discussions with Mike Blum, Tommaso Tesi and Fabio Trincardi. We are grateful to Gary Hampson, Whitney Autin, Paul Hudson and Christopher Esposito for their detailed and constructive comments which significantly improved the quality of our manuscript. This project was funded by ExxonMobil Upstream Research Company and by the Flagship Project RITMARE–The Italian Research for the Sea.

REFERENCES

Agenzia Interregionale Per Il Fiume Po (AIPO), 2005, Rilievo sezioni topografiche trasversali nella fascia B del Fiume Po, dalla confluenza con il Ticino al Mare. In Italian.

Amorosi, A., Maselli, V., and Trincardi, F., 2016, Onshore to offshore anatomy of a late Quaternary source-to-sink system (Po Plain-Adriatic Sea, Italy): Earth-Science Reviews, v. 153, p. 212-237.

Autorità di Bacino del Fiume Po (ADBPO), 2005, Programma generale di gestione dei sedimenti alluvionali dell'alveo del Fiume Po. Stralcio confluenza Tanaro-confluenza Arda. In Italian.

Autorità di bacino del fiume Po (ADBPO), 2008, Il recupero morfologico ed ambientale del fiume Po: Il contributo del Programma generale di gestione dei sedimenti del fiume Po. Diabasis, Reggio Emilia, Italy. ISBN 978-88-8103-561-8. In Italian.

Bernardi, D., Bizzi, S., Denaro, S., Dinh, Q., Pavan, S., Schippa, L., Soncini-Sessa, R., 2013. Integrating mobile bed numerical modelling into reservoir planning operations: the case study of the hydroelectric plant in Isola Serafini (Italy). WIT Transactions on Ecology and the Environment, v. 178, p. 63-75.

Biedenharn, D.S., Thorne, C.R., Soar, P.J., Hey, R.D., and Watson, Ch.C., 1999, A Practical Guide to Effective Discharge Calculation (Appendix A): U.S. Army Corps of Eng., Vicksburg, Mississippi, USA.

Blott, S.J., and Pye, K., 2001, Gradistat: a grain size distribution and statistics package for the analysis of unconsolidated sediments: Earth Surf. Process. Landf., v. 26, p. 1237-1248.

Blum, M.D., and Törnqvist, T.E., 2000, Fluvial responses to climate and sea-level change: a review and look forward: Sedimentology, v. 47, p. 2-48.

Blum, M.D., Martin, J., Milliken, K., and Garvin, 2013, Paleovalley systems: Insights from Quaternary analogs and experiments: Earth-Science Reviews, v. 116, p.128-169.

Bolla Pittaluga, M., Tambroni, N., Canestrelli, A., Slingerland, R.L., Lanzoni, S., and Seminara, G., 2015, When river and tide meet: The morphodynamic equilibrium of alluvial estuaries: Journal of Geophysical Research, v. 120, p. 75-94.

Brandt, S.A., 2000, Classification of geomorphological effects downstream of dams: Catena, v. 40, p. 375-401.

Bufe, A., Paola, C., and Burbank, D.W., 2016, Fluvial bevelling of topography controlled by lateral channel mobility and uplift rate: Nature Geoscience, v. 9, p. 706-710.

Cesi, 2004, Monitoraggio della qualità delle acque del nodo Po-Lambro. Anno 2003 Rapporto A4/000662 del 27 gennaio 2004. In Italian.

Chatanantavet, P., Lamb, M.P., and Nittrouer, J.A., 2012, Backwater controls of avulsion location on deltas: Geophysical Research Letters, v. 39, L01402.

Chen, J., Wang, Z., Li, M., Wei, T., and Chen, Z., 2012, Bedform characteristics during falling flood stage and morphodynamic interpretation of the middle-lower Changjiang (Yangtze) River channel, China: Geomorphology, v. 147-148, p. 18-26.

Chow, V.T., 1959, Open-channel hydraulics, McGraw-Hill, New York, p.680.

Church, M., 1995, Geomorphic response to river flow regulation: case studies and time-scales: Regulated Rivers: Research & Management, v. 11, p. 3-22.

Collier, M., Webb, R.H., and Schmidt, J.C., 1996, Dams and rivers: a primer on the downstream effects of dams: U.S. Geological Survey Circular, v. 1126, p. 1-94.

Colombera, L., Shiers, M.N., and Mountney, N.P., 2016, Assessment of backwater controls on the architecture of distributary channel fills in a tide-influenced coastal-plain succession: Campanian Neslen Formation, USA: Journal of Sedimentary Research, v. 86, p. 476-497.

Colombo, A., and Filippi, F., 2010, La conoscenza delle forme e dei processi fluviali per la gestione dell'assetto morfologico del fiume Po: Biologia Ambientale, v. 24, p. 331-348.

Cozzi, S., and Giani, M., 2011, River water and nutrient discharge in the Northern Adriatic Sea: current importance and long term changes: Continental Shelf Research, v. 31, p. 1881-1893.

Davide, V., Pardos, M., Diserebs, J., Ugazio, G., Thomas, R., and Dominik, J., 2003, Characterization of bed sediments and suspension of the river Po (Italy) during normal and high flow conditions: Water Research, v. 37, p. 2847-2864.

De Saint-Venant, A.J.C., 1871, Théorie du mouvement non permanent des eaux, avec application aux crues des rivières et a l'introduction de marées dans leurs lits. Comptes Rendus.

Domeneghetti, A., Carisi, F., Castellarin, A., Brath, A., 2015. Evolution of flood risk over large areas: Quantitative assessment for the Po river. Journal of Hydrology, v. 527, 809-823.

Edmonds, D.A., and Slingerland, R., 2006, Mechanics of river mouth bar formation: Implications for the morphodynamics of delta distributary networks: Journal of Geophysical Research, v. 112, F02034.

Edmonds, D.A., and Slingerland, R.L., 2009, Significant effect of sediment cohesion on delta morphology: Nature Geoscience, v. 3, p. 105-109.

Edmonds, D.A., Hoyal, D.C.J.D., Sheets, B.A., and Slingerland, R.L., 2009, Predicting delta avulsions: Implications for coastal wetland restoration: Geology, v. 37, p. 759-762.

Ferguson, R., Hoey, T., Wathen, S., and Werritty, A., 1996, Field evidence for rapid downstream fining in alluvial rivers: Journal of Geology, v. 106, p. 661-675.

Ferguson, R.I., 2003, Emergence of abrupt gravel to sand transitions along rivers through sorting processes: Geology, v. 31, p. 159-162.

Fernandes A.M., Törnqvist, T.E., Straub, K.M., and Mohrig, D., 2016, Connecting the backwater hydraulics of coastal rivers to fluvio-deltaic sedimentology and stratigraphy: Geology, v. 44, p. 979-982.

Ferrer-Boix, C., Chartrand, S.M., Hassan, M.A., Martin-Vide, J.P., and Parker, G., 2016, On how spatial variations of channel width influence river profile curvature: Geophysical Research Letters, v. 43, p. 6313-6323.

Franzoia, M., Nones, M., and Di Silvio, G., 2017, Long-term Morphodynamics of a Schematic River Analysed with a Zero-dimensional, Two-reach, Two-grainsize Model: Earth Surface Dynamics Discussion, doi:10.5194/esurf-2017-7.

Frings, R.M., 2008, Downstream fining in large sand-bed rivers: Earth-Science Reviews, v. 87, p. 39-60.

Geleynse, N., Storms, J.E.A., Walstra, D-J. R., Jagers, H.R., Wang, Z.B., and Stive, M.J.F., 2011, Controls on river delta formations; insights from numerical modelling: Earth and Planetary Science Letters, v. 302, p. 217-226.

Gibling, M.R., 2006, Width and thickness of fluvial channel bodies and valley fills in the geological record: a literature compilation and classification: Journal of Sedimentary Research, v. 76, p. 731-770.

Gibson, S.A., Park, J.H., and Fleming, M.J., 2010, Modeling Watershed and Riverine Sediment Processes with HEC-HMS and HEC-RAS: Watershed Management Conference 2010, p. 1340-1349, doi: 10.1061/41143(394)120.

Grant, G.E, Schmidt, J.C., and Lewis, S.L., 2003, A geological framework for interpreting downstream effects of dams on rivers, *in* O'Connor, J.E., and Grant, G.E., eds., A Peculiar River: Geology, Geomorphology, and Hydrology of the Dechutes River, Oregon 7, American Geophysical Union. Water Science and Applications, p. 209-225.

Graf, W.L., 2006, Downstream hydrologic and geomorphic effects of large dams on American rivers: Geomorphology, v. 79, p. 336-360.

Guerrero, M., and Lamberti, A., 2011, Flow field and morphology mapping using ADCP and multibeam techniques: Survey in the Po River: Journal of Hydraulic Engineering, v. 137, p. 1567-1587.

Guerrero, M., Di Federico, V., and Lamberti, A., 2013, Calibration of a 2-D morphodynamic model using water–sediment flux maps derived from an ADCP recording: Journal of Hydroinformatics, v. 15, p. 813-828.

Hirano, M., 1971, River bed degradation with armouring: Trans. of Jpn. Soc. Civ. Eng., v. 3, p. 194-195.

Hoey, T.B., and Ferguson, R., 1994, Numerical simulation of downstream fining by selective transport in gravel bed rivers: Model development and illustration: Water Resources Research, v. 30, p. 2251-2260.

Hoyal, D.C.J.D., and Sheets, B.A., 2009, Morphodynamic evolution of experimental cohesive deltas: Journal of Geophysical Research, v. 114, F02009.

Hudson, P.F., and Kesel, R.H., 2000, Channel migration and meander-bend curvature in the Lower Mississippi River prior to human modifications: Geology, v. 28, p. 531-534.

Ikeda, H., 1989, Sedimentary Controls on Channel Migration and Origin of Point Bars in Sand–Bedded Meandering Rivers, *in* Ikeda, S., and Parker, G., eds., River Meandering: American Geophysical Union, Washington, D.C. doi: 10.1029/WM012p0051

Kim, W., Petter, A., Straub, K., and Mohrig, D., 2014, Investigating the autogenic process response to allogenic forcing: experimental geomorphology and stratigraphy, *in* Martinius, A.W., Ravnås, R., Howell, J.A., Steel, R.J., and Womham, J.P., eds., Depositional Systems to Sedimentary Successions on the Norwegian Continental Margin: IAS Special Publication v. 46, Blackwell Publishing Ltd., Oxford, UK.

Jerolmack, D.J., and Swenson, J.B., 2007, Scaling relationships and evolution of distributary networks on wave-influenced deltas: Geophysical Research Letters, v. 34, L23402.

Jerolmack, D.J., 2009, Conceptual framework for assessing the response of delta channel networks to Holocene sea level rise: Quaternary Science Reviews, v. 28, p. 1786-1800.

Julien, P.Y., 1995, Erosion and sedimentation: Cambridge University Press, Cambridge, U.K.

Labrecque, P.A., Hubbard, S.M., Jensen, J.L., and Nielsen, H., 2011, Sedimentology and stratigraphic architecture of a point bar deposit, Lower Cretaceous McMurray Formation, Alberta, Canada: Bulletin of Canadian Petroleum Geology, v. 59, p. 147-171.

Lamb, M.P., Nittrouer, J.A., Mohrig, D., and Shaw, J., 2012, Backwater and river plume controls on scour upstream of river mouths: Implications for fluvio-deltaic morphodynamics: Journal of Geophysical Research, v. 117, F01002.

Lamberti, A., and Schippa, L., 1994, Studio dell'abbassamento del fiume Po: Previsioni trentennali di abbassamento a Cremona. Supplemento a Navigazione Interna, rassegna trimestrale di studi e informazioni: Azienda Regionale per i porti di Cremona e Mantova, Cremona, Italy. In Italian.

Lane, E.W., 1957, A study of the Channels Formed by Natural Streams Flowing in Erodible Material: U.S. Army Corps of Eng., Mo.River Div., Omaha, Nebraska.

Lanzoni, S., 2012, Evoluzione morfologica recente dell'asta principale del Po: Atti dei Convegni dei Lincei, Giornata Mondiale dell'Acqua, Accademia Nazionale dei Lincei. In Italian.

Lanzoni, S., Luchi, R., and Bolla Pittaluga, M., 2015, Modeling the morphodynamics equilibrium of an intermediate reach of the Po River (Italy): Advances in Water Resources, v. 81, p. 95-102.

Marchetti, M. 2002, Environmental changes in the central Po Plain (northern Italy) due to fluvial modifications and anthropogenic activities: Geomorphology, v. 44, p. 361-373.

Miall, A., 2014, Allogenic sedimentary controls, *in* Fluvial depositional systems: Springer International Publishing.

Montanari, A., 2012, Hydrology of the Po River: Looking for changing patterns in river discharge: Hydrol. Earth Syst. Sciences, v. 16, p. 3739-3747.

Moran, K.E., Nittrouer, J.A., Perillo, M.M., Lorenzo-Trueba, J., and Anderson, J.B., 2017, Morphodynamic modeling of fluvial channel fill and avulsion time scales during early Holocene transgression, as substantiated by the incised valley stratigraphy of the Trinity River, Texas: Journal of Geophysical Research, v. 122, p. 215-234.

Nittrouer, J.A., Allison, M.A., and Campanella, R., 2008, Bedform transport rates for the lowermost Mississippi River: Journal of Geophysical Research, v. 113, F03004.

Nittrouer, J.A., Mohrig, D., and Allison, M., 2011, Punctuated sand transport in the lowermost Mississippi River: Journal of Geophysical Research, v. 116, F04025.

Nittrouer, J.A., Shaw, J., Lamb, M.P., and Mohrig, D., 2012, Spatial and temporal trends for water-flow velocity and bed-material transport in the lower Mississippi River: Geol. Soc. Am. Bull., v. 124, p. 400-414.

Nones, M., Ronco, P., and Di Silvio, G., 2013, Modelling the impact of large impoundments on the Lower Zambezi River: Int. Journal of River Basin Management, v. 11, p. 221-236.

Nones, M., Pugliese, A., Domeneghetti, A., and Guerrero, M., 2018, Po River morphodynamics modelled with the open-source code iRIC, *in* Kalinowska, M., Mrokowska, M., and Rowiński, P., eds, Free Surface Flows and Transport Processes: GeoPlanet: Earth and Planetary Sciences, Springer, Cham, Switzerland, doi: 10.1007/978-3-319-70914-7_22.

Paola, C., and Seal, R., 1995, Grain size patchiness as a cause of selective deposition and downstream fining: Water Resources Research, v. 31, p. 1395-1407.

Paola, C., 2000, Quantitative models of sedimentary basin filling: Sedimentology, v. 47, p. 121-178.

Parker, G., Muto, T., Akamatsu, Y., Dietrich, W.E., and Wesley Lauer, J., 2008, Unravelling the conundrum of river response to rising sea-level from laboratory to field. Part II. The Fly-Strickland River system, Papua New Guinea: Sedimentology, v. 55, p. 1657-1686.

Petts, G.E., 1979, Complex response of river channel morphology subsequent to reservoir construction: Progress in Physical Geography, v. 3, p. 329-362.

Sambrook Smith, G.H., and Ferguson, R.I., 1995, The gravel to sand transition along river channels: Journal of Sedimentary Research, v. A65, p. 423-430.

Samuels, P.G., 1989, Backwater length in rivers: Proceedings of Institution of Civil Engineers, Part 2, v. 87, p. 571-581.

Schumm, S.A., and Stevens, M.A., 1973, Abrasion in place: a mechanism for rounding and size reduction of coarse sediments in rivers: Geology, v. 1, p. 37-40.

Schumm, S.A., 1981, Evolution and response of the fluvial system: sedimentologic implications: Soc. Econ. Paleont. Mineral. Spec. Pub., v. 31, p. 19-29.

Schumm, S.A., 1993, River response to baselevel change: Implications for sequence stratigraphy: Journal of Geology, v. 101, p. 279-294.

Shields, A., 1936, Application of similarity principles and turbulence research to bed-load movement: Soil Conservation Service.

Shanley, K.W., McCabe, P.J., and Hettinger, R.D., 1992, Tidal influence in Cretaceous fluvial strata from Utah, USA: a key to sequence stratigraphic interpretation: Sedimentology, v. 39, p. 905-930.

Shaw, J.B., and McElroy, B., 2016, Backwater number scaling of alluvial bed forms: Journal of Geophysical Research, v. 121, p. 1436-1455.

Simon, A., and Collison, A.J.C., 2002, Quantifying the mechanical and hydrologic effects of riparian vegetation on streambank stability: Earth Surf. Process. Landforms, v. 27, p. 527-546.

Snyder, N.P., Rubin, D.M., Alpers, C.N., Childs, J.R., Curtis, J.A., Flint, L.E., and Wright, S.A., 2004, Estimating accumulation rates and physical properties of sediment behind a dam: Englebright Lake, Yuba River, northern California: Water Resources Research, v. 40, W11301.

Southard, J.B., and Boguchwal, L.A., 1990, Bed configuration in steady unidirectional water flows. Part 2. Synthesis of flume data: Journal of Sedimentary Petrology, v. 60, p. 658-679.

Sturn, T.W., 2010, Open channel hydraulics, New York, McGraw-Hill.

Syvitski, J.P.M., and Kettner, A.J., 2007, On the flux of water and sediment into the Northern Adriatic Sea: Continental Shelf Research, v. 27, p. 296-308.

Surian, N., and Rinaldi, M., 2003, Morphological response to river engineering and management in the alluvial channels in Italy: Geomorphology, v. 50, p. 307-326.

Thorne, C.R., 1990, Effects of vegetation on riverbank erosion and stability, *in* Thornes, J.B., eds, Vegetation and Erosion: Processes and Environments, John Wiley & Sons, p.125-144,

US Army Corps of Engineers, 2015, HEC-RAS River Analysis System, 2D Modeling User's Manual, Version 5.0.

Van Heijst, M.W.I.M., and Postma, G., 2001, Fluvial response to sea-level changes: a quantitative analogue, experimental approach: Basin Research, v. 13, p. 269-292.

Van Rijn, L.C., 1984, Sediment transport, Part I: Bed Load Transport: Journal of Hydraulic Engineering, v. 110, p. 1412-1430.

Venditti, J.G., and Church, M., 2014, Morphology and controls on the position of a gravel-sand transition: Fraser River, British Columbia: Journal of Geophysical Research, v. 119, p. 1959-1976.

White, W.R., Meyer Peter, E., Rottner, J., Ackers, P., Milli, H., Muller, R., Bishop, A., Hansen, E., Crabbe, A., Einstein, H., and Bagnold, R., 1975, Sediment transport theories: Proc. of the Institution of Civil Engineers, v. 59, p. 265-292.

Wickert, A.D., Martin, J.M., Tal, M., Kim, W., Sheets, B., and Paola, C., 2013, River channel lateral mobility: metrics, time scales, and controls: Journal of Geophysical Research, v. 118, p. 396-412.

Williams, G.P., and Wolman, M.G., 1984, Downstream effects of dams on alluvial rivers: U.S. Geol. Surv. Prof. Pap., v. 1286, p. 1-83.

Wright, S., and Parker, G., 2005, Modeling downstream fining in sand-bed rivers. II: application: Journal of Hydraulic Research, v. 43, p. 621-631.

Zanchettin, D., Traverso, P., and Tomasino, M., 2008, Po River discharges: a preliminary analysis of a 200-year time series: Climate Change, v. 89, p. 411-433.

Figure Captions

Figure 1. Po River course and its catchment basin, with reported the main tributaries entering the river in the study area (black square). Point B marks the location of the Isola Serafini dam. DEM derived from SRTM 90m (available at http://www.cgiar-csi.org/data/srtm-90m-digital-elevation-database-v4-1).

Figure 2. Top: Aerial view of the study area derived from a combination of two images (date 7/21/2004 and 5/8/2005, left and right sides of the white dashed line, respectively) acquired during low flow conditions, see figure 4 for details. Blue lines (numbered from 1 to 14) represent the location of river cross sections acquired in 1954. Note that section 14 is just downstream of the dam. Red dots (named from A to V) mark the location of the boreholes presented in figure 9. Orange squares (named from “alpha” to “delta”) highlight the location of the multibeam bathymetric sections presented in figure 10. The blue star marks the location of the gauging station near the city of Piacenza. Bottom: thalweg elevation derived from the 2005 multibeam bathymetric survey (MB, red line; source AIPO, 2005), from the 1954 river cross sections (blue squares) and from the 2000 river cross sections (green square). The numbers in blue refer to the cross sections, as in the map. Yellow arrows mark the location of the four main tributaries (Tidone, Lambro, Trebbia and Nure rivers).

Figure 3. Schematic representation of the Isola Serafini dam (A, front view), with later views during low flow discharge events (backwater river profile and the gates are closed, B) and during high discharge events (drawdown river profile and the gates open depending of the discharge, C).

Figure 4. Top: water surface elevation (blue) and water discharge (red) data during June-September 2014; cruise time is reported below. Bottom: water surface elevation of the Po River during the acquisition of the aerial views presented in Figure 2; both images are acquired during low flow conditions (black squares).

Figure 5. Top: extent of the Po River surface area obtained from five aerial surveys since 1954 (before the construction of the Isola Serafini dam). Bottom: close view (age reported in years) of four-selected meander loops (1 to 4 moving downstream). In detail: orange and yellow arrows in meander loop 1 indicate channel bar and point bar accretion over time, respectively; blue arrows in

meander loop 2 mark river banks with increasing vegetation cover; red arrows in meander loop 2, 3 and 4 highlight channel bars that are progressively eroded until disappear.

Figure 6. Lateral migration rate of the Po River centerline, calculated in four time intervals, plotted to distance upstream.

Figure 7. Detailed view of meander loops 1, 3 and 4 (see location in figure 4) showing the grain-size variability of river bed sediment. Blue (sediment < 0.063mm), yellow (sediment between 0.063-2 mm) and red (>2 mm).

Figure 8. Morphology of the Po River along the final reaches located upstream of the Isola Serafini dam in 1954 and 2005. River bed samples acquired in this study are represented with coloured dots and are reported on the 2005 satellite image (each colour refers to a specific sediment sample). Red dots (named from K to V) mark the location of the boreholes presented in figure 9.

Figure 9. Schematic representation of the lithology of the boreholes available in the area (see location in figure 2). Note the presence of extensive coarse-grained deposit for the entire section investigated.

Figure 10. 3-D images of the river bed derived from the multibeam bathymetric survey of AIPO and 2-D bathymetric sections (red lines). The multibeam data are located in figure 2. The 3-D images are selected to highlight the bedforms pattern observed in different river reaches.

Figure 11. Variability of river bed sediment along the 70-km-long reach upstream of the Isola Serafini dam (blue dots, dimensions scale with D_{50} grain sizes). Vertical blue bars represent the range of grain sizes, while horizontal bars their spatial distribution along the river. Red diamonds

represent the average dune length derived from 300 m long 2D profiles extracted from the multibeam bathymetry. Vertical red bars represent the maximum and minimum dune length in each transect.

Figure 12. Simulated water surface profiles (left) and bottom shear stresses (right) calculated at different water discharges along the 70-km-long river reach of the study area.

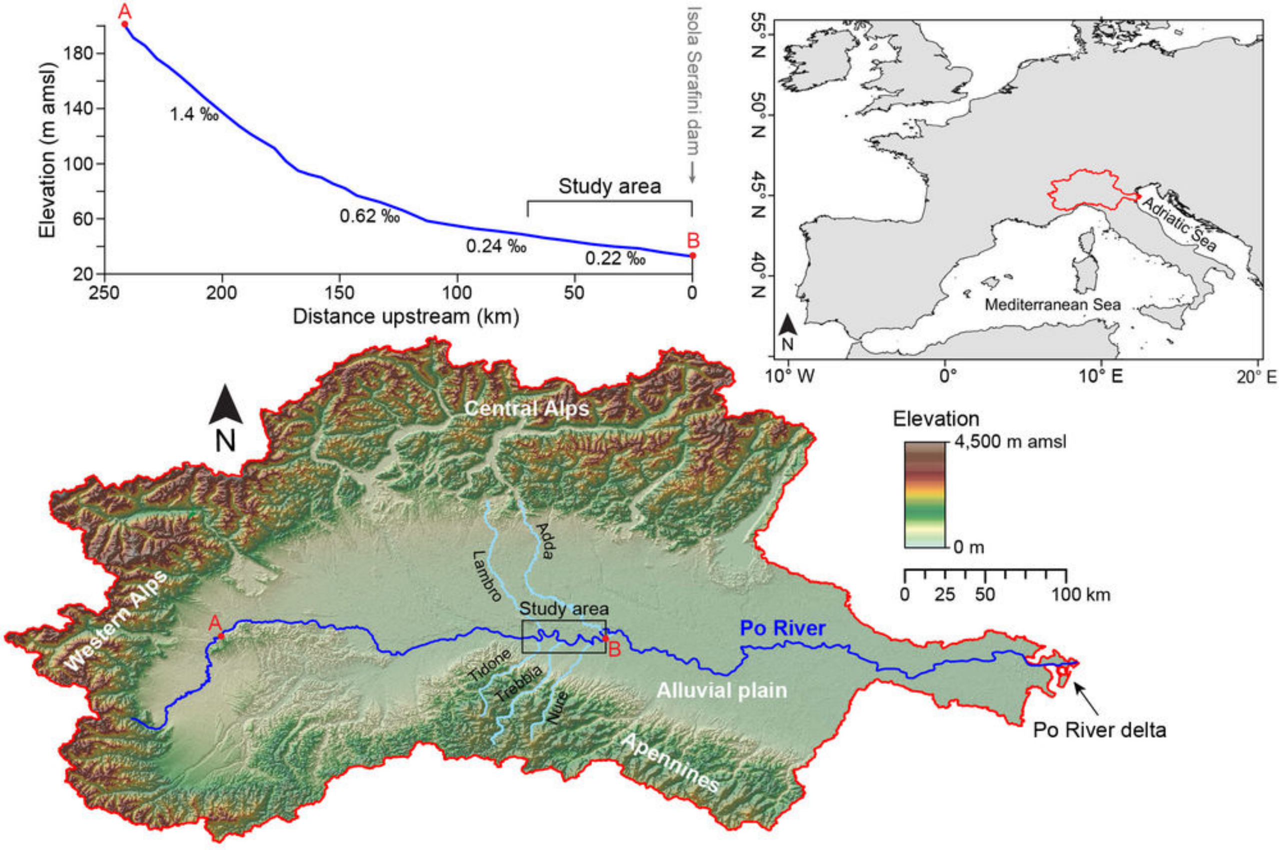

A
B
Isola Serafini dam
Study area
1.4 ‰
0.62 ‰
0.24 ‰
0.22 ‰
Elevation (m amsl)
180
140
100
60
20
250
200
150
100
50
0
Distance upstream (km)
55° N
50° N
45° N
40° N
10° W
0°
10° E
20° E
Adriatic Sea
Mediterranean Sea
N
N
Central Alps
Western Alps
Adda
Lambro
Study area
A
B
Po River
Tidone
Trebbia
Nure
Alluvial plain
Apennines
Po River delta
Elevation
4,500 m amsl
0 m
0
25
50
100 km

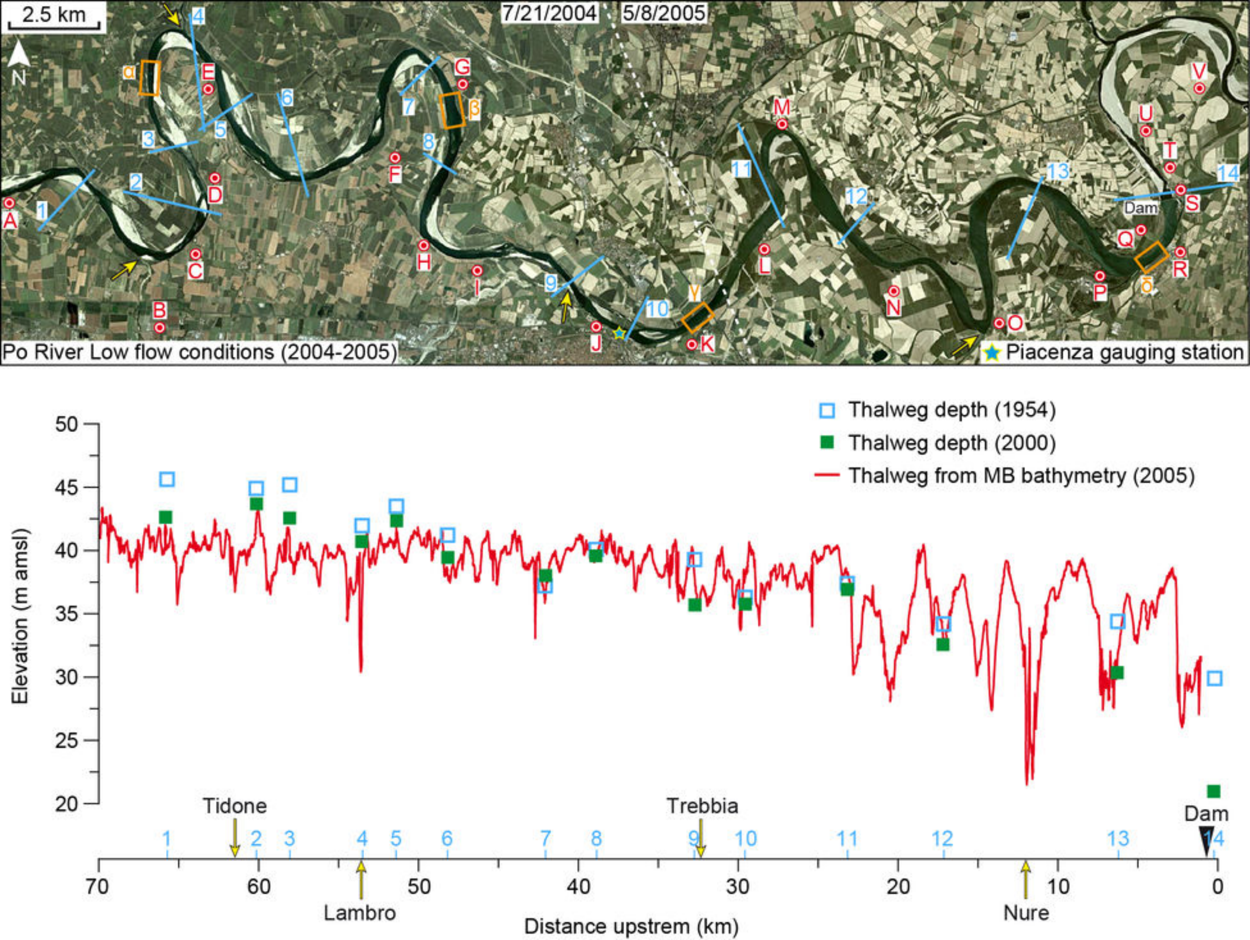

2.5 km
N
7/21/2004
5/8/2005
Po River Low flow conditions (2004-2005)
Piacenza gauging station
Dam
Thalweg depth (1954)
Thalweg depth (2000)
Thalweg from MB bathymetry (2005)
Elevation (m amsl)
Distance upstrem (km)
Tidone
Lambro
Trebbia
Nure
Dam

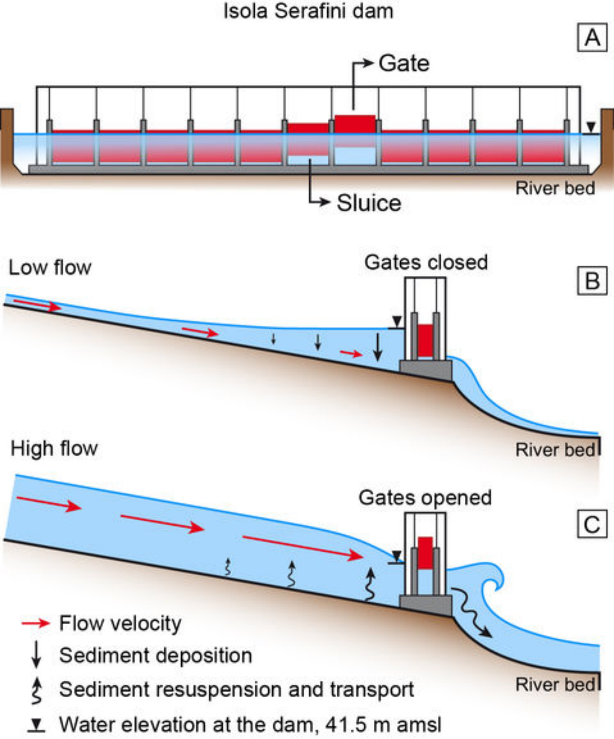
Isola Serafini dam
A
Gate
Sluice
River bed
Low flow
Gates closed
B
River bed
High flow
Gates opened
C
River bed
Flow velocity
Sediment deposition
Sediment resuspension and transport
Water elevation at the dam, 41.5 m amsl

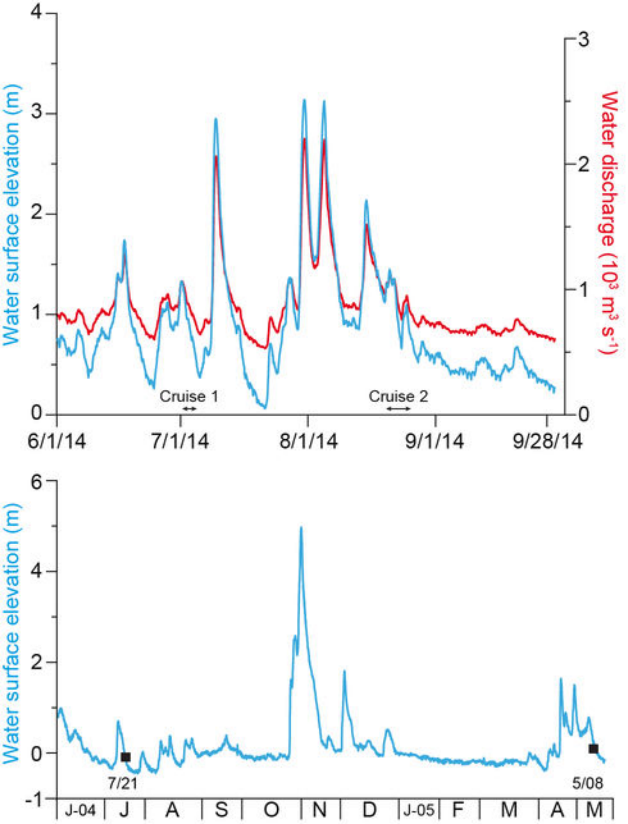
Water surface elevation (m)
Water discharge (10³ m³ s⁻¹)
Cruise 1
Cruise 2
6/1/14
7/1/14
8/1/14
9/1/14
9/28/14
Water surface elevation (m)
7/21
5/08
J-04
J
A
S
O
N
D
J-05
F
M
A
M

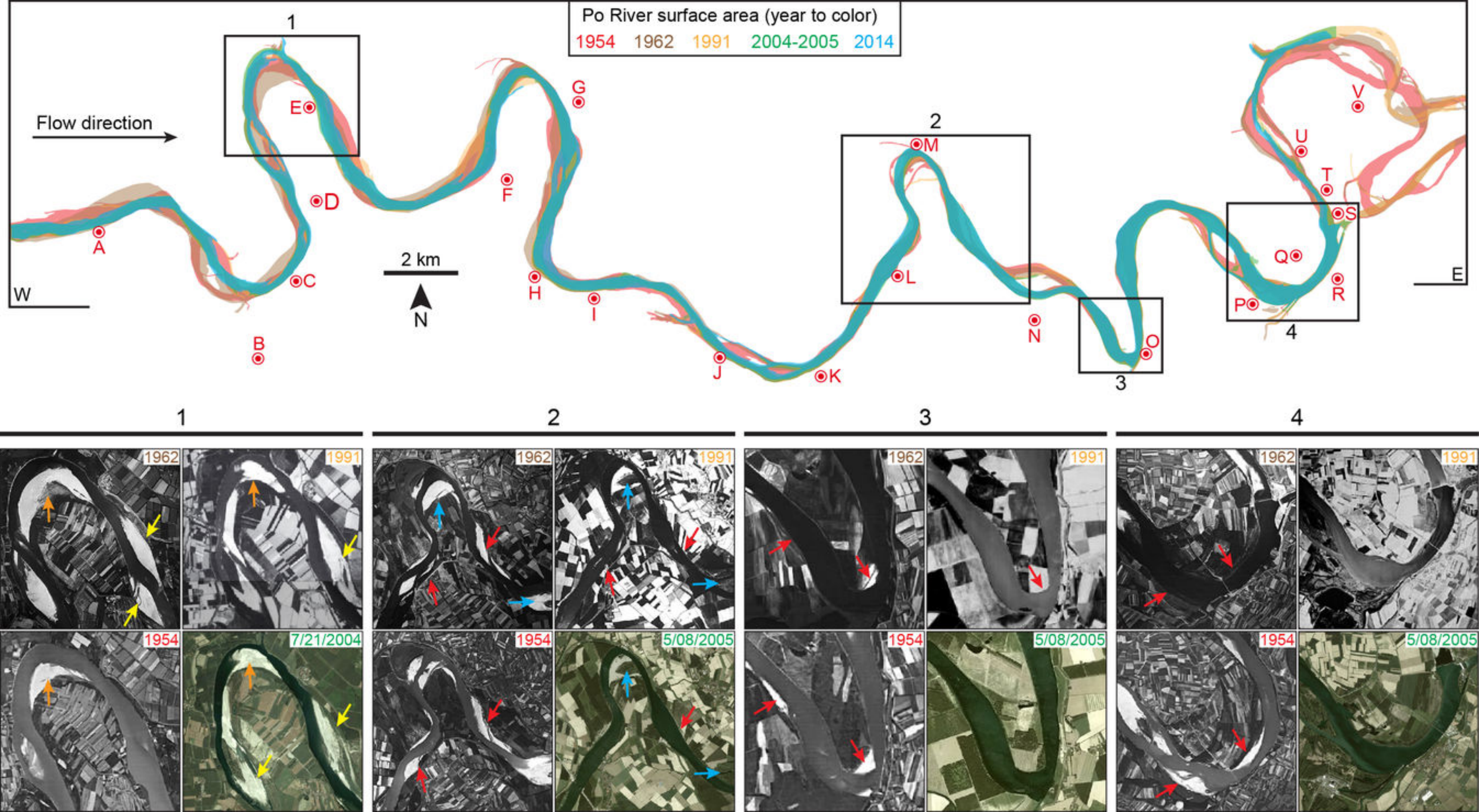
Po River surface area (year to color)
1954 1962 1991 2004-2005 2014
Flow direction
W
E
2 km
N
A
B
C
D
E
F
G
H
I
J
K
L
M
N
O
P
Q
R
S
T
U
V
1
2
3
4
1962
1991
1954
7/21/2004
5/08/2005

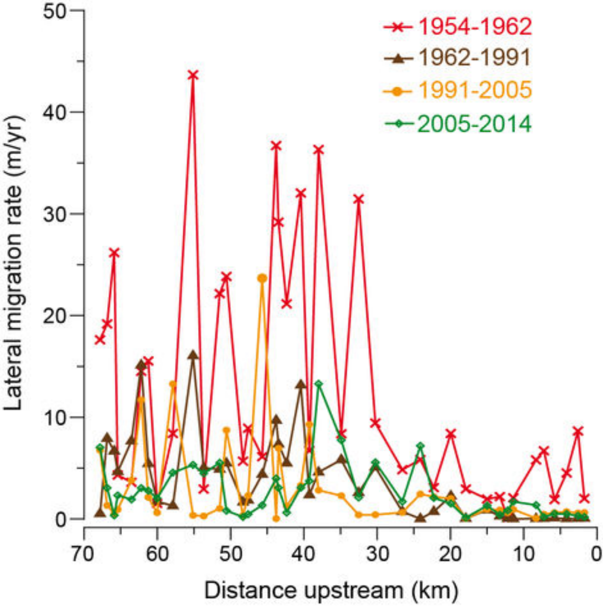

1954-1962
1962-1991
1991-2005
2005-2014
Lateral migration rate (m/yr)
50
40
30
20
10
0
70
60
50
40
30
20
10
0
Distance upstream (km)

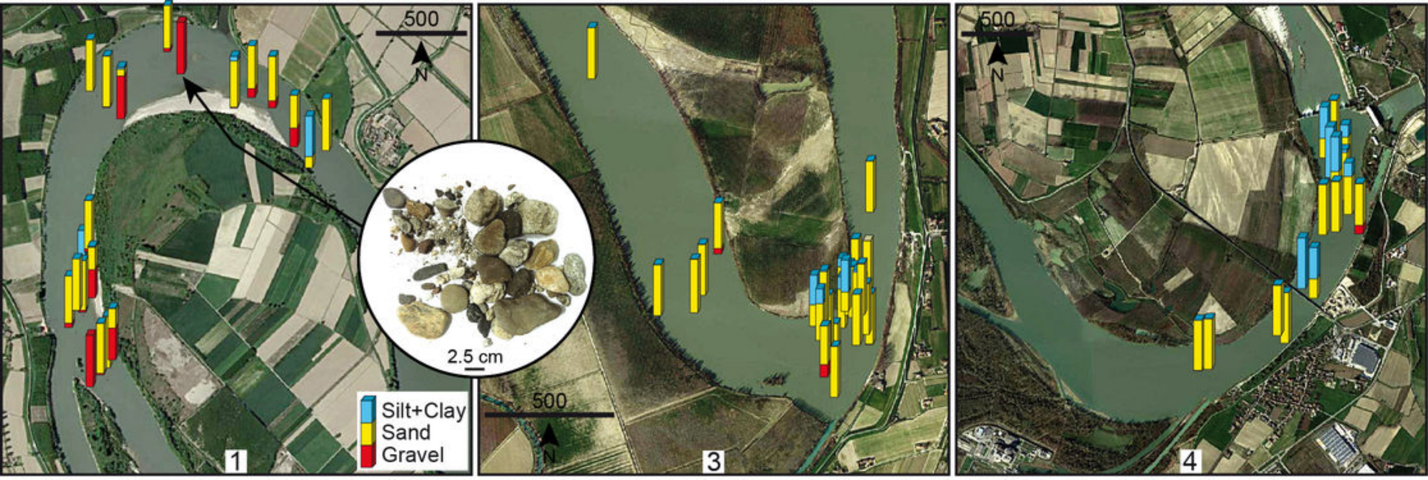
500
N
2.5 cm
Silt+Clay
Sand
Gravel
1
500
N
3
500
N
4

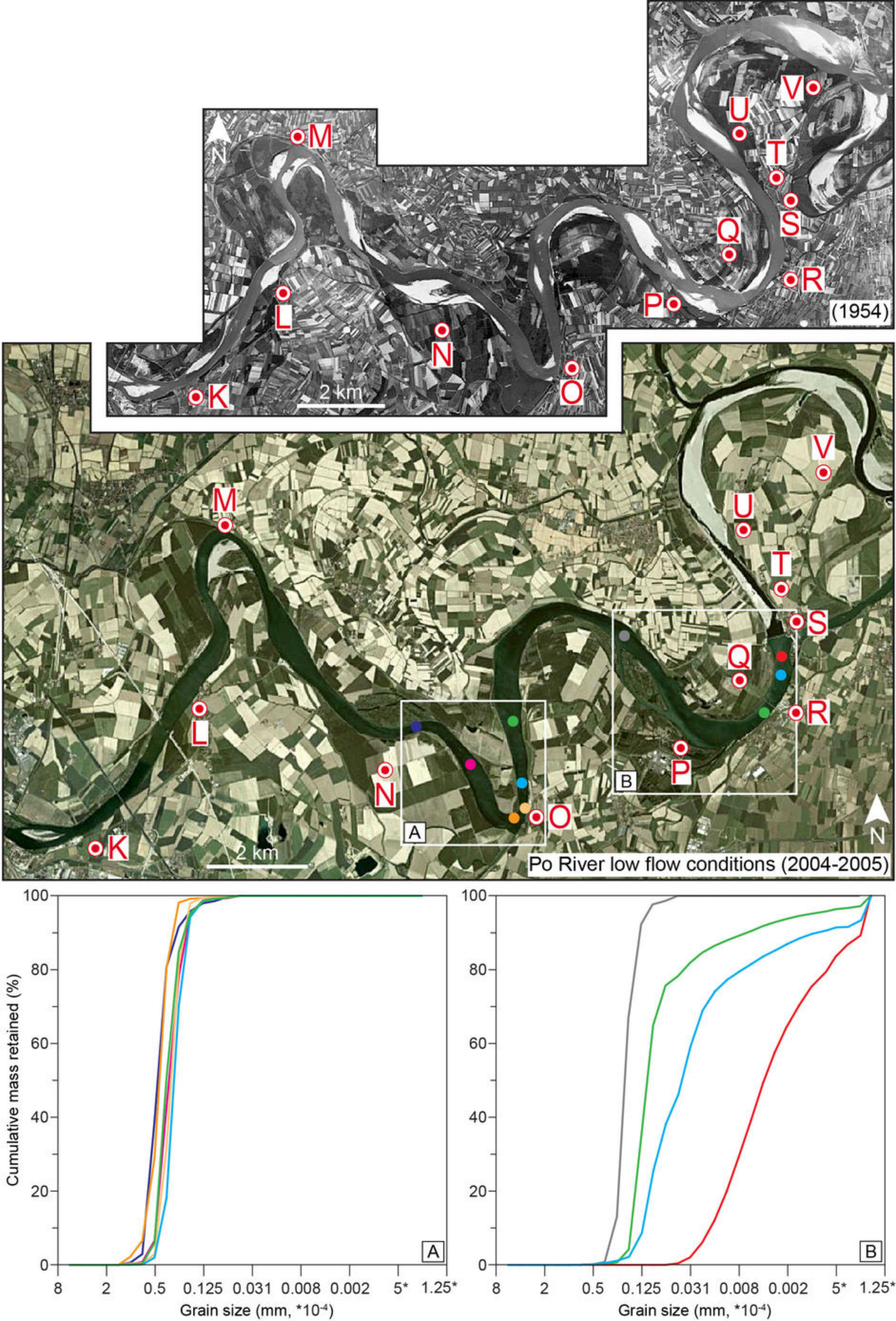

M
U
V
T
S
Q
R
P
L
N
O
K
2 km
(1954)
N
M
V
U
T
S
Q
R
L
P
B
N
O
A
K
2 km
Po River low flow conditions (2004-2005)
N
Cumulative mass retained (%)
100
80
60
40
20
0
8
2
0.5
0.125
0.031
0.008
0.002
5*
1.25*
Grain size (mm, *10⁻⁴)
A
B

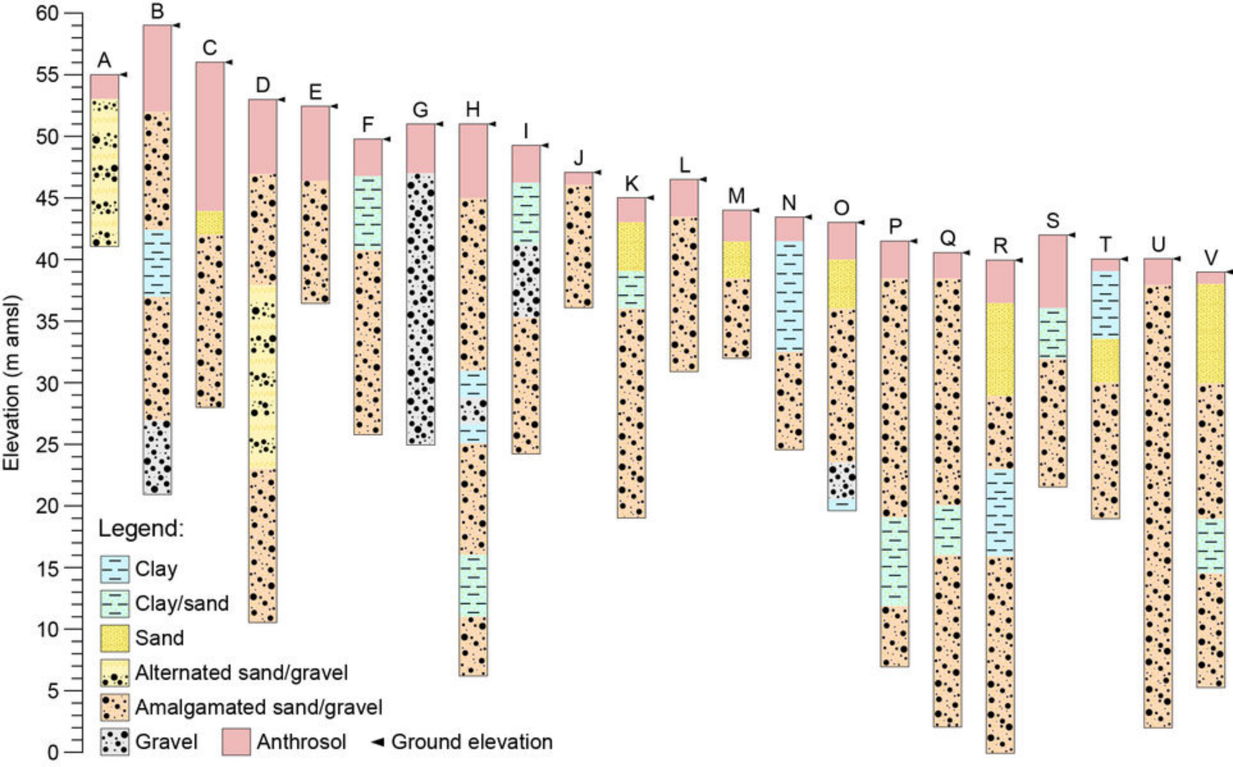

Elevation (m amsl)
0
5
10
15
20
25
30
35
40
45
50
55
60
A
B
C
D
E
F
G
H
I
J
K
L
M
N
O
P
Q
R
S
T
U
V
Legend:
Clay
Clay/sand
Sand
Alternated sand/gravel
Amalgamated sand/gravel
Gravel
Anthrosol
Ground elevation

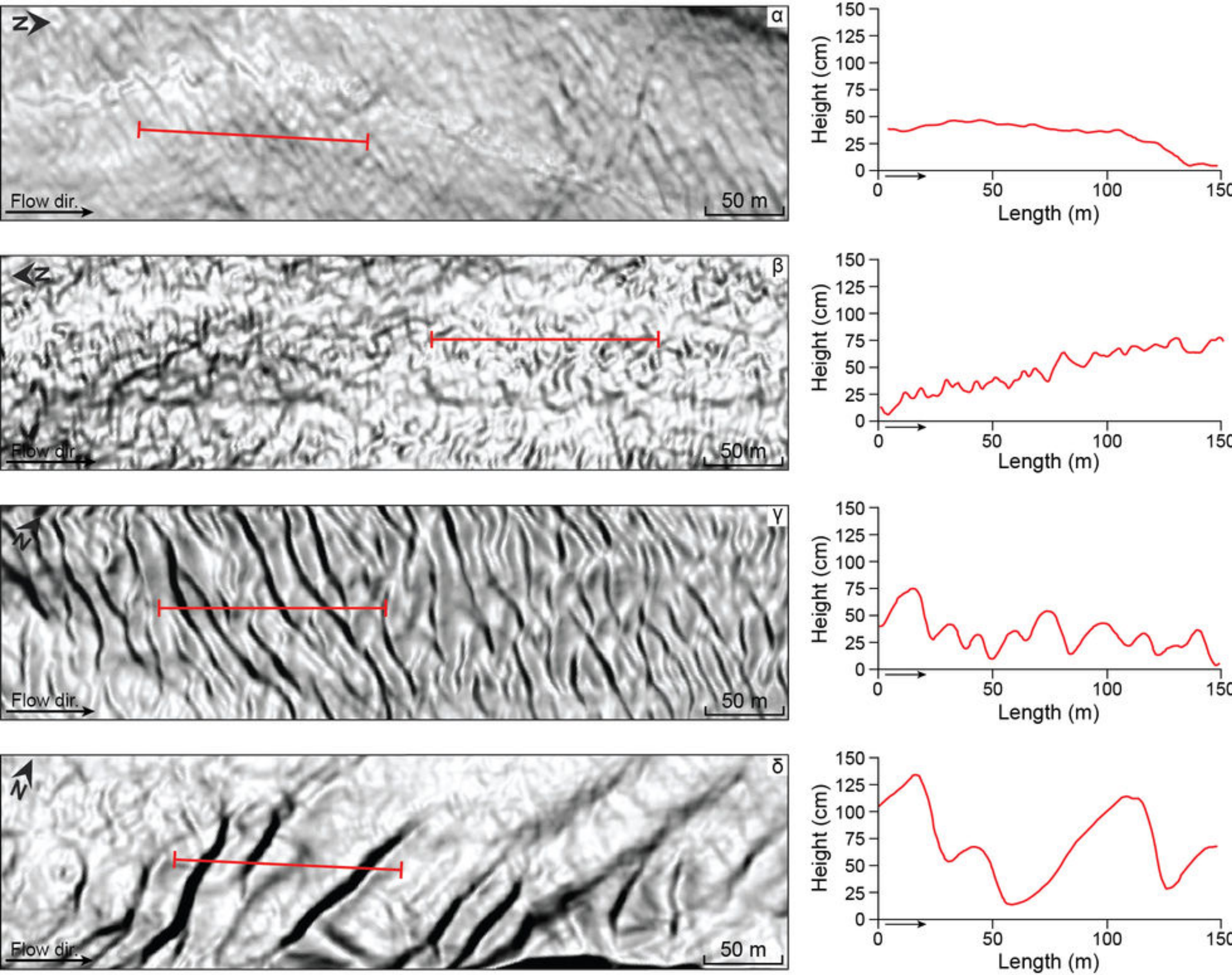
α
Flow dir.
50 m
Height (cm)
Length (m)
β
Flow dir.
50 m
Height (cm)
Length (m)
γ
Flow dir.
50 m
Height (cm)
Length (m)
δ
Flow dir.
50 m
Height (cm)
Length (m)

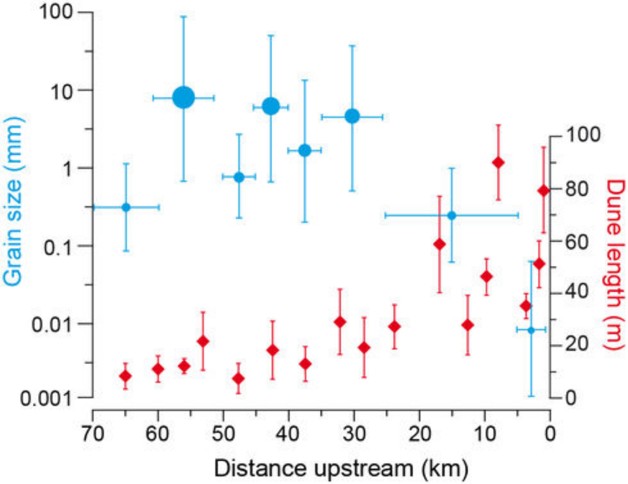
100
10
1
0.1
0.01
0.001
Grain size (mm)
100
80
60
40
20
0
Dune length (m)
70
60
50
40
30
20
10
0
Distance upstream (km)

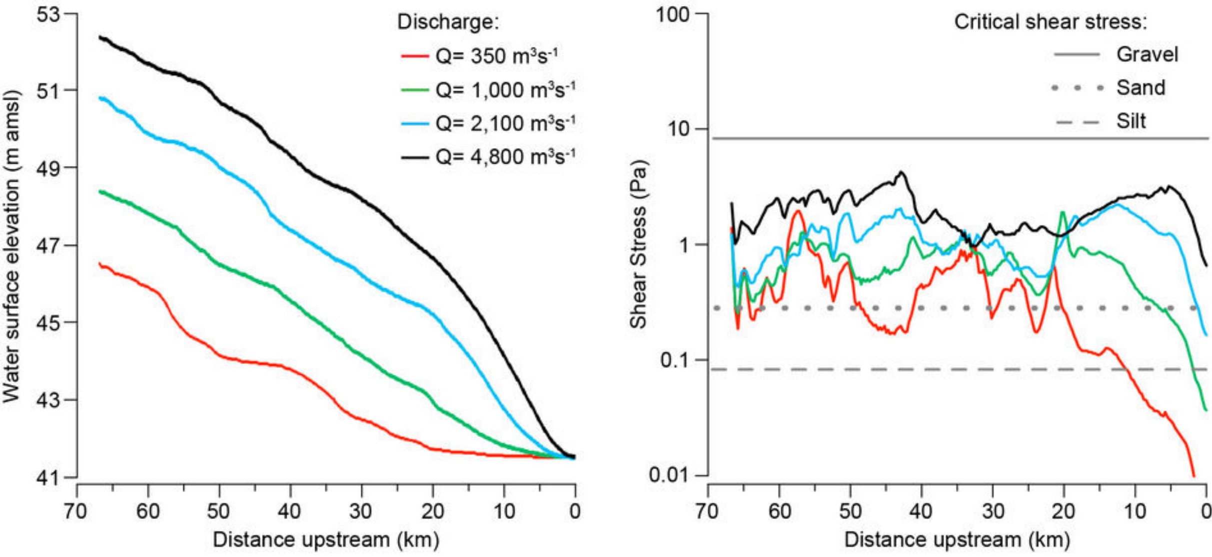

Discharge:
Q= 350 m³s⁻¹
Q= 1,000 m³s⁻¹
Q= 2,100 m³s⁻¹
Q= 4,800 m³s⁻¹
Water surface elevation (m amsl)
53
51
49
47
45
43
41
70
60
50
40
30
20
10
0
Distance upstream (km)
Critical shear stress:
Gravel
Sand
Silt
Shear Stress (Pa)
100
10
1
0.1
0.01
70
60
50
40
30
20
10
0
Distance upstream (km)

Table 1. Critical shear stress by particle-size classification (modified from Julien, 1995).

particle classification	*particle diameter* [mm]	*Shield parameter* [-]	*critical shear stress* [Pa]
coarse cobble	128 – 256	0.054 – 0.054	112 – 223
fine cobble	64 – 128	0.052 – 0.054	53.8 – 112
very coarse gravel	32 – 64	0.05 – 0.052	25.9 – 53.8
coarse gravel	16 – 32	0.047 – 0.05	12.2 – 25.9
medium gravel	8 – 16	0.044 – 0.047	5.7 – 12.2
fine gravel	4 – 8	0.042 – 0.044	2.7 – 5.7
very fine gravel	2 – 4	0.039 – 0.042	1.3 – 2.7
very coarse sand	1 – 2	0.029 – 0.039	0.47 – 1.3
coarse sand	0.5 – 1	0.033 – 0.029	0.27 – 0.47
medium sand	0.25 – 0.5	0.048 – 0.033	0.194 – 0.27
fine sand	0.125 – 0.25	0.072 – 0.048	0.145 – 0.194
very fine sand	0.0625 – 0.125	0.109 – 0.072	0.110 – 0.145
coarse silt	0.0310 – 0.0625	0.165 – 0.109	0.0826 – 0.110
medium silt	0.0156 – 0.0310	0.25 – 0.165	0.0630 – 0.0826
fine silt	0.0078 – 0.0156	0.3 – 0.25	0.0378 – 0.0630